# Supporting information

# Microwave-assisted synthesis followed by a reduction step: making persistent phosphors with a large storage capacity

*José Miranda de Carvalho,[1,2,*] David Van der Heggen,[1,] Lisa I.D.J. Martin,[1,] Philippe F. Smet[1,*]*

1. Lumilab, Department of Solid-State Sciences, Ghent University, Krijgslaan 281, S1, 9000 Gent, Belgium.

2. Institute of Physics, University of São Paulo, BR-05508-900, São Paulo-SP, Brazil.

## Synthesis details

The X-ray powder diffraction patterns can be used to qualitatively discuss the mechanism of the material's formation using the MASS method. For the MASS synthesis, the dielectric heating process occurs first in the microwave susceptor (carbon), which is reaching temperatures close to 1000 °C after a few minutes of MW irradiation. Due to the incomplete burning of the carbon at high temperatures, *in-situ* CO gas is formed and acts as a reducing local atmosphere reducing the $Eu^{3+}$ to $Eu^{2+}$ in the synthesis. Also, the carbon surface can act as a $CO_2$ converter, by the Boudouard reaction.[1] The carbon used as initial absorber can also participate in the formation of

the $Sr_2MgSi_2O_7$ by shifting the equilibrium to the decomposition of carbonates as shown in Eq. 1 and 2:

$$SrCO_3(s) \rightarrow SrO(s) + CO_2(g) \quad (1)$$

$$CO_2(g) + C(s) \rightarrow 2\,CO(g) \quad (2)$$

During the heating process, the carbonates will decompose and form $CO_2(g)$ as a by-product, which will react with the carbon surface of the surroundings generating the CO(g). At high temperatures, the formation of CO gas is favored, therefore, consuming the $CO_2$ gas formed by the decomposition of $SrCO_3$.[1]

In this work, MASS synthesis was calibrated to run at the same temperature as the conventional synthesis (~ 1250 °C) in order to compare the thermal and non-thermal effects of the microwave irradiation. Evidence of the non-thermal effect of microwave irradiation can be associated with the swift synthesis times; the MASS method yields $Sr_2MgSi_2O_7$ materials in a mere 22 minutes process, whereas the conventional solid-state process needs *ca.* 8-10 hours in total to obtain the same structure with comparable impurity levels. The electromagnetic radiation exerting ponderomotive forces are of the same magnitude, or even more significant than the conventional convective heating, adding an additional component in the mass transport in the crystal. The microwave effect can be especially significant in the grain boundaries, where most of the solid-state reactions are known to begin.[2]

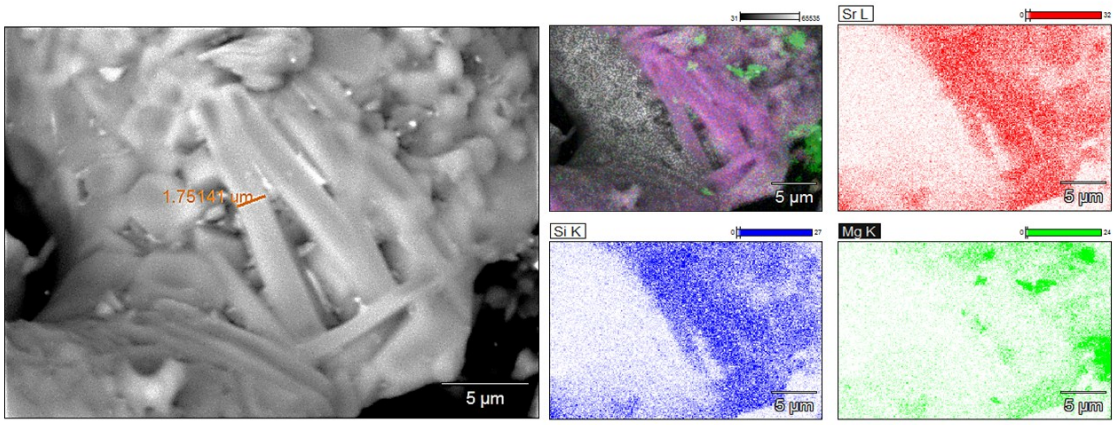


**Figure S1**. SEM-EDX mapping of the $Sr_2MgSi_2O_7$ microrod structures formed in the MASS synthesis. The mapping shows the individual contributions from the Sr (red), Si (blue), and Mg (green) atoms, and a superimposed image of summed contributions.

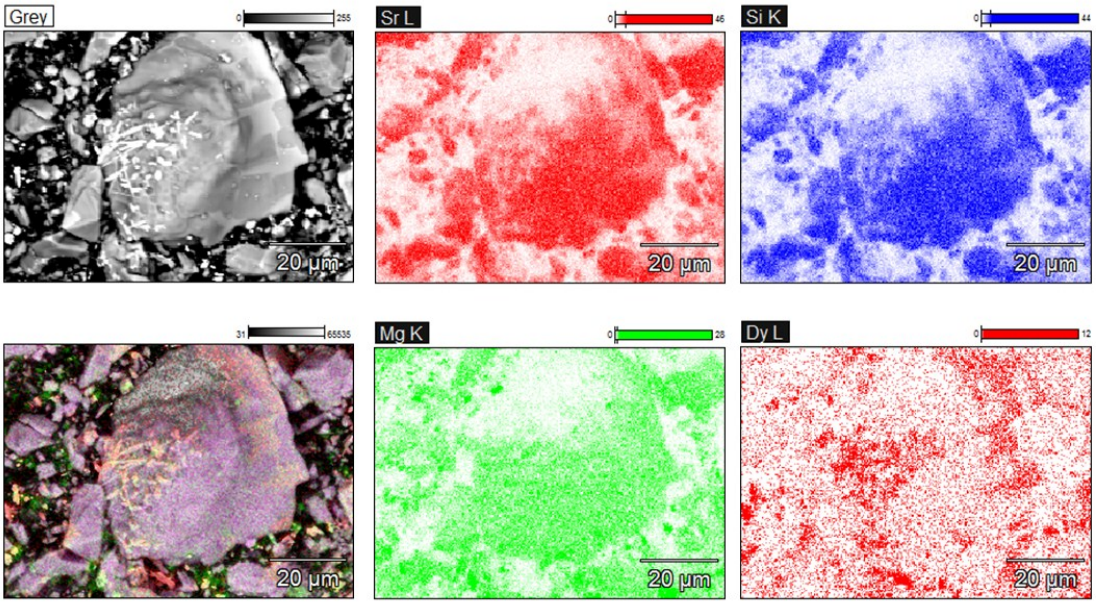


**Figure S2**. SEM-EDX mapping of the $Sr_2MgSi_2O_7$:$Eu^{2+}$(1%), $Dy^{3+}$(10%) materials obtained by MASS synthesis. The mapping shows the individual contributions from the Sr (red), Si (blue), and Mg (green) atoms, and a superimposed image of summed contributions. The superimposed image indicates that the segregated wires are composed mainly by Dy and Mg.

The luminous efficacy and the average photon energy can be obtained considering the curve for human eye sensitivity V(λ). Since the photon counting method assumes the normalization of the emitted photons by the luminous efficacy and average photon energies, the total storage capacity can give an unambiguous comparison of different materials with different emitted photon energies. The luminous efficacy of the emission spectra was found to be 137 lm/W. The average photon energy was also calculated and found to be 2.56 eV for all materials. One can have in mind that the storage capacity can have a source of errors, such as variations in the luminous efficacy and the average photon energy as a function of time, which was not taken into consideration in our measurements. However, minor changes are expected for both parameters when considering only one emitting center ($Eu^{2+}$) that has only one emission band ($4f^{6}5d^{1} \rightarrow 4f^{7}$) in the visible spectral range.

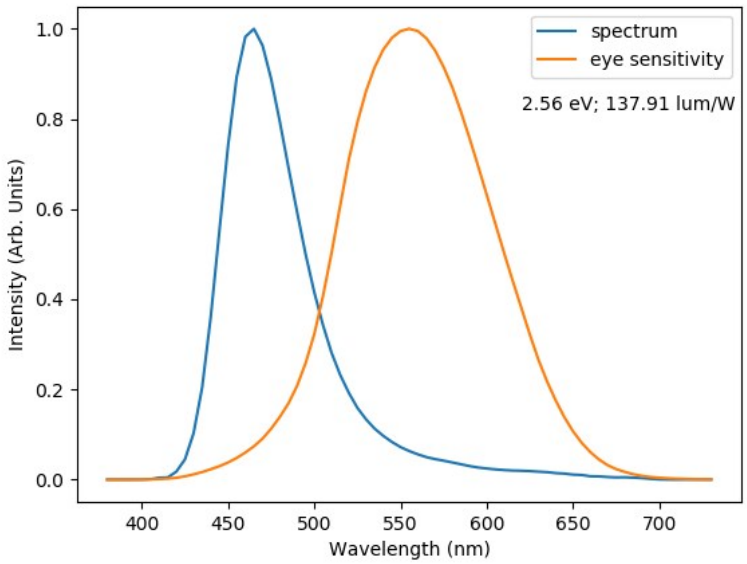


**Figure S3.** Emission spectra of exemplary $Sr_2MgSi_2O_7:Eu^{2+},Dy^{3+}$ material (blue curve). Eye sensitivity curve, V(λ), (orange curve). The curves were used to calculate the average photon energy and the luminous efficacy used in the photon counting experiments.[3]

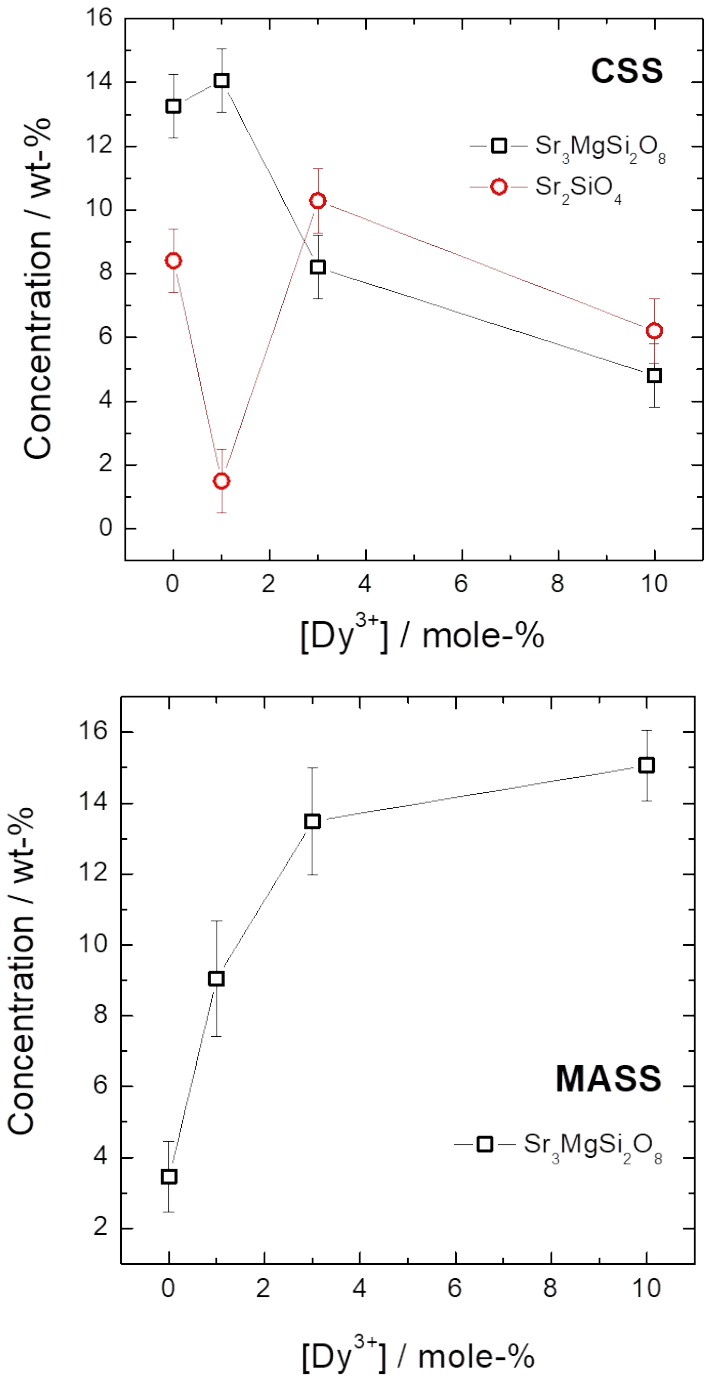


**Figure S4.** Impurities concentration calculated by Rietveld analysis of the $Sr_2MgSi_2O_7$ materials with different $Dy^{3+}$ concentration. The error bars are 10 times the error calculated with the GSAS program.

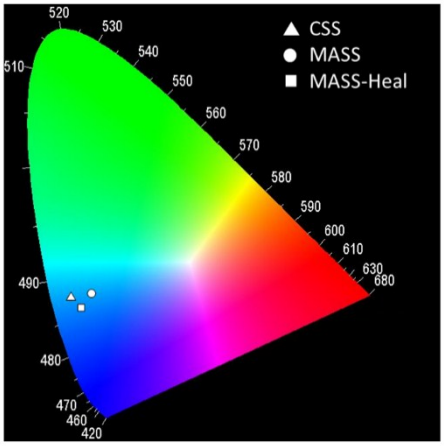


**Figure S5**. Steady-state emission spectra CIE diagram of the $Sr_2MgSi_2O_7:Eu^{2+},Dy^{3+}$ (1 mole-%) materials obtained by the CSS, MASS and MASS-Heal methods.

**Table S1**. Rietveld refinement parameter of the $Sr_2MgSi_2O_7$ materials with different $Dy^{3+}$ concentration obtained by both CSS and MASS synthesis.

| | Undoped | | Eu; Dy (1; 1 mole-%) | | Eu; Dy (1; 3 mole-%) | | Eu; Dy (1; 10 mole-%) | |
|---|---|---|---|---|---|---|---|---|
| **$Sr_2MgSi_2O_7$**[a] | MASS[b] | CSS[c] | MASS[d] | CSS[e] | MASS[f] | CSS[g] | MASS[h] | CSS[i] |
| Crystal system | Tetragonal | Tetragonal | Tetragonal | Tetragonal | Tetragonal | Tetragonal | Tetragonal | Tetragonal |
| Space group | $P\bar{4}2_1m$ | $P\bar{4}2_1m$ | $P\bar{4}2_1m$ | $P\bar{4}2_1m$ | $P\bar{4}2_1m$ | $P\bar{4}2_1m$ | $P\bar{4}2_1m$ | $P\bar{4}2_1m$ |
| Z | 2 | 2 | 2 | 2 | 2 | 2 | 2 | 2 |
| Lattice parameter *a,* Å | 7.9878(4) | 7.9969(4) | 7.9967(5) | 7.9949(3) | 7.9816(5) | 7.9943(2) | 7.9840(3) | 8.0036(5) |
| Lattice parameter c, Å | 5.1699(4) | 5.1635(2) | 5.1755(5) | 5.1640(3) | 5.1528(6) | 5.1553(2) | 5.1518(3) | 5.1616(3) |
| *a/c* | 1.5450(5) | 1.5487(3) | 1.5451(5) | 1.5481(2) | 1.5489(5) | 1.5507(4) | 1.5497(5) | 1.5506(3) |
| Cell volume, Å3 | 329.87(2) | 329.86(2) | 330.96(3) | 330.07(4) | 328.26(2) | 329.46(3) | 328.40(2) | 330.63(2) |
| $\chi^2$ | 3.12 | 2.17 | 3.55 | 4.22 | 5.19 | 5.23 | 5.07 | 6.48 |

***a***. PDF n° 01-075-1736. ***b***. Figure of Merit ($R_{wp}$, $R_p$) values: 10.48%, 7.60%. ***c***. Figure of Merit ($R_{wp}$, $R_p$) values: 10.77%, 7.64%. ***d***. Figure of Merit ($R_{wp}$, $R_p$) values: 13.5%, 8.68%. ***e***. Figure of Merit ($R_{wp}$, $R_p$) values: 13.33%, 8.58%. ***f***. Figure of Merit ($R_{wp}$, $R_p$) values: 14.9%, 9.50%. ***g***. Figure of Merit ($R_{wp}$, $R_p$) values: 15.77%, 10.45%. ***h***. Figure of Merit ($R_{wp}$, $R_p$) values: 15.8%, 10.2%. ***i***. Figure of Merit ($R_{wp}$, $R_p$) values: 16.24%, 10.96%.

**REFERENCE**


[1] J. Hunt, A. Ferrari, A. Lita, M. Crosswhite, B. Ashley, A.E. Stiegman, Microwave-specific enhancement of the carbon-carbon dioxide (boudouard) reaction, J. Phys. Chem. C. 117 (2013) 26871–26880. doi:10.1021/jp4076965.

[2] S.A. Freeman, J.H. Booske, R.F. Cooper, Modeling and numerical simulations of microwave-induced ionic transport, J. Appl. Phys. 83 (1998) 5761–5772. doi:10.1063/1.367432.

[3] D. Van der Heggen, J.J. Joos, D.C. Rodríguez Burbano, J.A. Capobianco, P.F. Smet, Counting the photons: Determining the absolute storage capacity of persistent phosphors, Materials (Basel). 10 (2017) 1–13. doi:10.3390/ma10080867.